MRI AND GRAVIMETRIC STUDIES OF HYDROLOGY IN DRIP IRRIGATED HEAPS AND ITS EFFECT ON THE PROPAGATION OF BIOLEACHING MICRO-ORGANISMS

Authors

Marijke A Fagan* [a,b]

marijke.fagan-endres@uct.ac.za

I Emmanuel Ngoma [b]

emmanuel.ngoma@uct.ac.za

Rebecca A Chiume [b]

Sanet Minnaar [b]

sanetminnaar@hotmail.com

Andrew J Sederman [a]

ajs40@cam.ac.uk

Michael L Johns [c]

michael.johns@uwa.edu.au

Susan TL Harrison [b]

sue.harrison@uct.ac.za

[a] Department of Chemical Engineering and Biotechnology, University of Cambridge, Pembroke Street, Cambridge, CB2 3RA, UK

[b] Centre for Bioprocess Engineering Research, Department of Chemical Engineering, University of Cape Town, Rondebosch, 7701, South Africa, Tel: +27 21 6502759

[c] School of Mechanical and Chemical Engineering, University of Western Australia, 35 Stirling Highway, Crawley, WA 6009, Australia

* Corresponding author

ABSTRACT

Heap bioleaching performance is dependent on the contacting of the leach solution with the ore bed, hence on the system hydrodynamics. In this study two experimental setups were used to examine hydrodynamics associated with irrigation from a single drip emitter, one of the most common methods of heap irrigation. A specialist magnetic resonance imaging (MRI) method which is insensitive to the metal content of the ore was used to examine the liquid flow into an ore bed in the immediate vicinity of an irrigation point. The distribution of liquid in, microbial colonisation of and mineral recovery from a bioleach of a large scale 132 kg "ore slice" were subsequently monitored using sample ports positioned along the breadth and height of the reactor. In both systems the lateral movement of the liquid increased with bed depth, though preferential flow was evident. The majority of the liquid flow was in the region directly below the irrigation point and almost no liquid exchange occurred in the areas of lowest liquid content at the upper corners of the bed in which fluid exchange was driven by capillary action. The MRI studies revealed that the liquid distribution was unchanging following an initial settling of the ore bed and that, at steady state, the majority (~60%) of the liquid flowed directly into established large channels. The limited lateral movement of the liquid had a significant impact on the local leaching efficiencies and microbial colonisation of the ore with cell concentrations in the regions of lowest liquid content lying below the detection limit. Hence poor lateral liquid distribution with drip irrigation, and the associated impact on colonisation was identified as a significant disadvantage of this irrigation approach. Further, the need to optimise fluid exchange throughout the ore bed was identified as key for optimisation of leaching performance.

Keywords: Bioleaching, hydrology, irrigation, MRI, colonisation, sulfide ores

1 INTRODUCTION

Heap bioleaching systems are unsaturated ore beds, typically stacked using agglomerated ore that are irrigated with lixiviant from the top of the bed. Most are also aerated from the base, to provide sufficient oxygen and carbon dioxide for microbial growth. Iron and/or sulfur oxidising micro-organisms, found attached to the ore surface or as planktonic cells in the liquid, are used to facilitate the oxidation of base metal sulfides in the ore. The result of the leaching reactions is that the metal ions (e.g. Cu^{2+}) are liberated into the leach solution. They are subsequently transported out of the heap and recovered from the effluent pregnant leach solution (PLS) which exits at the base of the heap. The heap hydrology therefore plays two key roles as both reaction and transport medium. These determine the degree of recovery that is possible in an ore bed because contact is required between the leach solution and the exposed mineral surfaces on the ore particles for the leaching reactions to occur (Rossi, 1990).

Liquid flow in heaps is controlled variably by gravitational and capillary forces as a result of the particle size distribution in heaps ranging from sub-millimetre to multiple centimetres (Ilankoon and Neethling, 2012). This, coupled with the highly inhomogeneous structure of the ore beds which is another feature of the wide particle size distribution, means that existing models of hydrodynamics in similar well-described chemical systems, such as trickle bed reactors, do not adequately describe the heaps. Most heap bioleaching hydrology studies have considered the use of tracers to extract hydrodynamic parameters and develop models of the liquid flow (Bouffard and Dixon, 2001; De Andrade Lima, 2006) or to study the issue of preferential flow resulting from the inhomogeneous heap structure (Decker and Tyler, 1999; O'Kane Consultants Inc., 2000; Wu et al., 2007) for which analogies to unsaturated soil hydrodynamics have proved particularly successful. However, the liquid distribution within a heap from a drip irrigation point, one of the most common methods of irrigation (Bartlett, 1998; Kappes, 2002), has not been examined in any specific detail.

Inoculation of heaps is also often achieved or subvented via the drip irrigation points. Transportation of the micro-organisms to exposed sites on the mineral surface is known to be by convective transport due to fluid flow, diffusive transport as a result of Brownian motion and active movement by chemotaxis in which the micro-organisms move in response to a chemical concentration gradient (Rossi, 1990; van Loosdrecht et al., 1990). Consequently the propagation of the micro-organisms throughout the heap would be expected to be a strong

function of the liquid distribution. While many studies have considered microbial attachment to mineral surfaces, for example Rodriguez et al. (2003), Ghauri et al. (2007) and Africa et al. (2010), the effect of heap hydrodynamics on the propagation of micro-organisms to locations favourable for growth and biooxidation and on microbial attachment/detachment is not known.

This study therefore focuses on the liquid distribution and resulting microbial propagation in agglomerated chalcopyrite ore beds that are drip irrigated from a single emitter source. In the first instance, a specialist magnetic resonance imaging (MRI) method which is insensitive to the metal content of the ore (Fagan et al., 2013; Fagan et al., 2012) is used to examine the liquid flow in the immediate vicinity of the irrigation point where the signal in an MRI acquisition is directly proportional to the liquid volume. The liquid distribution is subsequently monitored using gravimetric techniques in a long-term bioleach of a 132 kg "slice" of agglomerated ore, the results of which are related to the microbial colonisation and mineral recovery in the heap.

2 MATERIALS AND METHODS

2.1 MRI cell

The cell used in the MRI experiments (Figure 1) had the liquid inlet point positioned centrally at the top of the bed, thereby avoiding wall effects. The small size of the system meant that no influence on the liquid distribution by other emitters was possible. Low grade copper ore (2.95% Fe, 0.69% Cu and 2.02% S by weight, mineral breakdown given in Table 1, particle size distribution specified in Figure 2) was agglomerated using 50 mL deionised H_2O/kg ore and 3.7 mL concentrated H_2SO_4/kg ore. Approximately 1 kg was packed on top of a layer of 10 mm glass ballotini placed on top of the drainage plate to provide a liquid disengagement region below the ore which prevented upwards wicking of any liquid. The cell was irrigated at a flow rate of 10 mL/h (approximately equivalent to 1 L/m^2.h) with deionised water that had been doped with 0.8 g/L of $GdCl_3.6H_2O$ in accordance with the MRI signal requirements (Fagan et al., 2012). Multiple ore samples were tested in order to examine the reproducibility of the results.

The MRI was performed on a Bruker AV 85, 2 T horizontal bore spectrometer with a wide bore radio frequency coil (inner diameter of 83 mm). A standard SESPI sequence was used as described in Fagan et al. (2012). The field of view was 80 mm × 80 mm in the x and y

directions and 160 mm in the z (along the bore length) and the nominal resolution in all three directions was 2.5 mm. 2D projections were acquired at 4, 15, 30 and 60 minutes once irrigation had started, followed by hourly scans. This was continued until an approximate steady state was reached at which time a 3D image was acquired.

In the first series of experiments it was desired to test the repeatability of an irrigation experiment. For this a bed of agglomerated ore was drip irrigated from an initially dry state on three occasions (A, B and C). The first run, A, was the first time that the agglomerated ore sample was irrigated following the sample preparation. B and C were subsequent irrigations that were performed after allowing the bed to dry out. Two agglomerated ore samples (1 and 2) were tested.

A proton-MRI inactive D_2O tracer was used as a tracer in a second set of experiments performed on a further two agglomerated ore samples (I and II). In the first run, A, the ore had been agglomerated with D_2O and was irrigated from an initially wet state with the $GdCl_3$ doped water. For run B, the same ore was dried overnight and then re-irrigated with the $GdCl_3$ doped water. This was done for a minimum of 24 hours after which the feed solution was swapped to D_2O. The disappearance of the MRI signal as the D_2O flowed into the ore bed was recorded in run C.

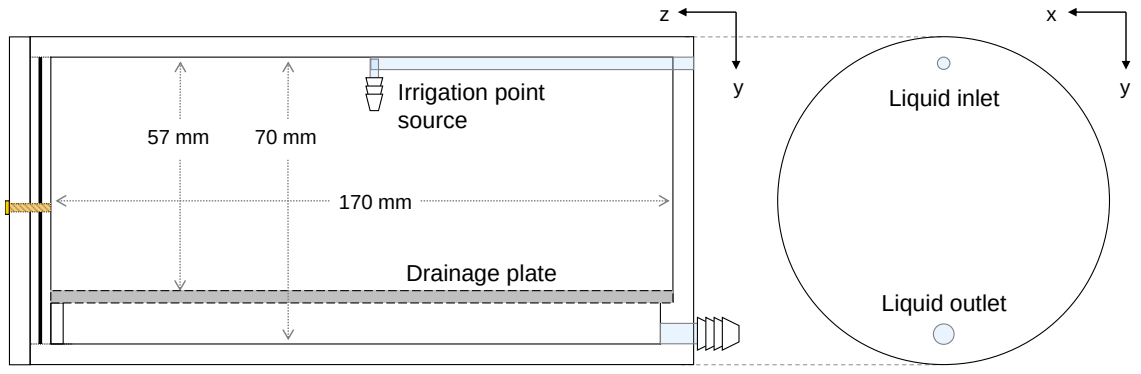

Figure 1. Illustration of the cylindrical horizontal cell used for the MRI experiments.

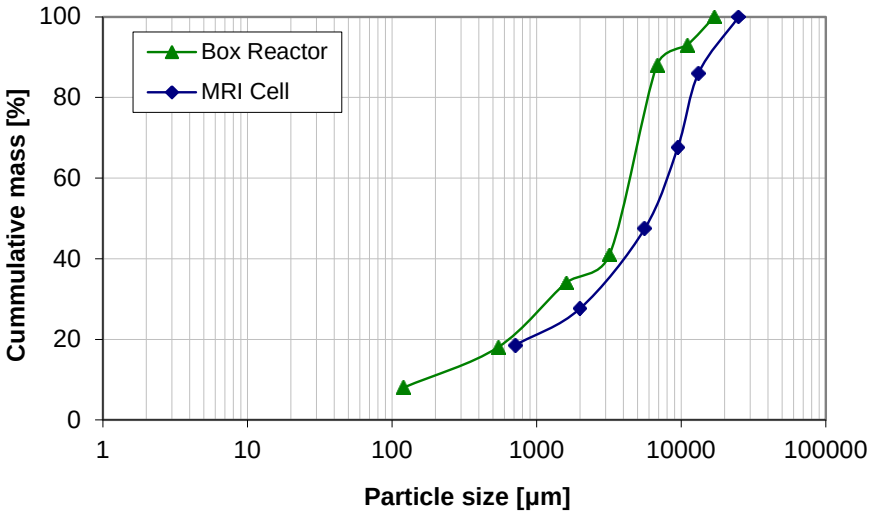

Figure 2. Particle size distribution of the ore used in the MRI cell and the box reactor experiments.

Table 1. Major mineral contributions to the available copper and pyrite content in the low grade copper-bearing ore sample.

Copper Source	% Contributed to Cu content	% in Ore
Chalcopyrite	28.4	0.196
Chalcocite	41.8	0.288
Covellite	6.7	0.046
Bornite	15.1	0.104
Pyrite	-	1.7

2.2 Bioleach "ore-slice" box reactor

The "ore-slice' box reactor depicted in Figure 3 was packed with 132 kg of low grade copper ore (particle size distribution given in Figure 2) agglomerated with 50 mL deionised H_2O/kg ore and 3.7 mL concentrated H_2SO_4/kg ore, as used in the MRI experiments. The reactor had multiple irrigation point options, 13 drainage ports at the base and in-bed sampling ports located on the face in a 13×26 matrix.

After an initial wetting process and a 26 day preparatory acid wash (pH 1.15), the bed was inoculated on day 27 via irrigation at a rate of 6 L/m^2.h from the single point source on the extreme left of the bed as indicated in Figure 3. A mixed mesophilic culture containing *Acidithiobacillus ferrooxidans*, *At. thiooxidans*, *At. caldus*, and predominantly *Leptospirillum ferriphilum*, confirmed by qPCR, at 10^{12} cells/ton was used. The ore bed was irrigated

continuously at 6 L/m^2.h with a liquid feed of composition: 0.5 g/L ferrous sulfate ($FeSO_4.7H_2O$), 183.3 mg/L $(NH_4)_2SO_4$, 60.5 mg/L $NH_4H_2PO_4$, and 111.2 mg/L K_2SO_4 in deionised water, adjusted to pH 1.15. The bed was additionally aerated at 1.75 L/min (supplied in excess) and was operated at ambient conditions.

The moisture content was measured across nine zones of the ore bed (Figure 3) on day 24, 49, 63 and 83 from the sample ports by drying 20 g samples of the wet ore to find the weight percentage of the sample that was liquid. The cell densities of the samples were assessed using cell counts. The percolating solution was collected daily through 13 drainage ports at the reactor base and the pH, redox potential and iron and copper concentrations were quantified. The iron and copper concentration measurements were done using the 1,10-phenanthroline colorimetric method (Komadel and Stucki, 1988) and atomic absorption spectroscopy, respectively.

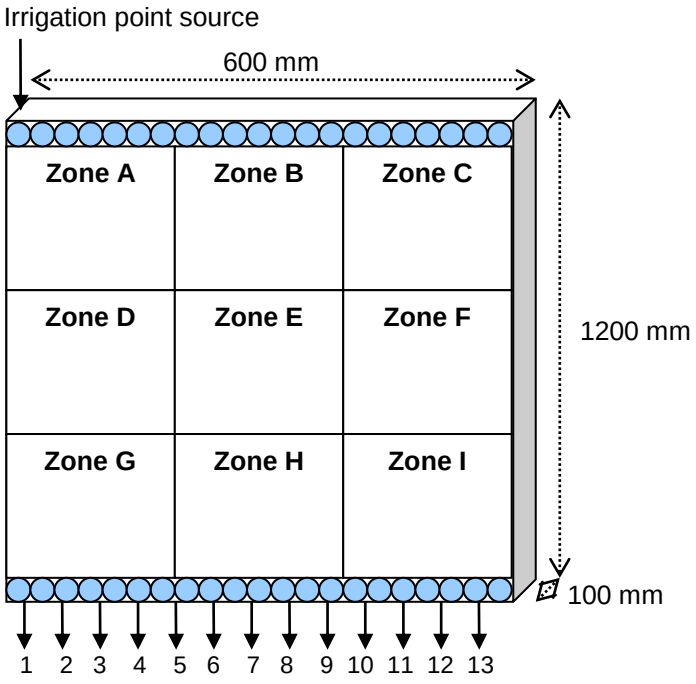

Figure 3. Schematic of the "ore-slice" box reactor that was drip irrigated from a single point at the top left.

3 RESULTS AND DISCUSSION

3.1 MRI cell

3.1.1 Repeat irrigation of agglomerated ore

The 2D y-z projections for the three irrigation cycles (A, B and C) of the agglomerated ore samples 1 and 2 are presented in Figures 4 and 5. The images were thresholded at the same signal magnitude level and combined to compare the liquid distributions, the results of which are shown in Table 2.

In the first sample, the horizontal movement of the liquid in run A_1 was as extensive as the downward movement during the first 60 minutes of irrigation. At the 30 minute mark the liquid extended approximately 27.5 mm to the left, 10 mm to the right and 35 mm down from the liquid entry point. This extended to 32.5 mm, 25 mm and 42.5 mm respectively after 60 minutes. This indicates that there was strong capillary suction within the agglomerated ore bed which enabled the lateral transport of the liquid. The vertical infiltration rate, driven by gravity, was slightly higher. Horizontal movement of the liquid was also present in runs B_1 and C_1; here there was preferential flow to the right side of the sample rather than to the left.

In the second run, the cell was packed with a fresh, representatively split ore sample. The liquid flow during the first 30 minutes of irrigation was relatively symmetrical in run A_2, with only a slight bias to the right side of the cell. After 30 minutes the liquid had travelled 42.5 mm down from the drip point and a maximum of 22.5 mm and 20 mm to the right and left of the drip point. The liquid reached the bottom of the ore at this time and so only changes in the horizontal movement of the liquid were observed thereafter. The downwards flow of the liquid under gravity was therefore more dominant for this sample than the horizontal movement due to capillary suction in run A_1. Some flow variation between ore samples is expected as the larger ore particles in agglomerated samples introduce a high degree of heterogeneity to the bed. After 30 minutes in runs B_2 and C_2 the liquid had traversed 40 mm down, 12.5 mm right and 25 mm left. Hence the liquid distribution in this case displayed a preference towards the left of the drip point. This was more pronounced than in run A_2 which indicates that there was a change in the capillary suction following the initial irrigation cycle. The rate of the downwards flow of the liquid was unaffected from the initial irrigation of the ore.

Therefore the liquid distribution in run A was different to the results of the later runs (B and C) for both samples. In the case of the first sample less than half of the liquid followed the same flow path for the first 30 minutes of irrigation. The effect was less pronounced for the irrigation of the second sample where less than half of the liquid followed the same flow path for the first 15 minutes, and there was only 60% agreement in the liquid distribution at 30 minutes. By contrast, only minor differences developed between the liquid flow paths in runs B and C. This is particularly evident in the second sample, where more than three quarters of the liquid followed the same path in runs B and C throughout the experiment. The initial differences in the liquid distributions across the three runs become insignificant by the 180th minute in both samples at which stage the entire ore bed was wet. In a larger sample the differences in the liquid distribution would be expected to extend further into the ore bed.

Both ore beds were also observed to slump during the first irrigation run: by 12 mm for the first bed and 5 mm for the second bed. No further slumping of the bed occurred with subsequent irrigation in the later runs. This behaviour is common in both lab scale experiments and full scale operation of heaps (Bouffard and Dixon, 2001; Lin et al., 2005). Therefore the change in the liquid path following the initial wetting of the sample may be attributed to some of the finer ore particles having shifted during the first irrigation of the ore, thereby causing the liquid to wick into a different part of the ore bed. The movement of fines is a common phenomenon in heap leaching and has been reported to result in areas of lower voidage developing where the fines accumulate towards the base of columns (Lin et al., 2005) as well as plugging of void spaces in some extreme cases (Bartlett, 1998). The results consequently illustrate that changes in the structure of the packed ore due to slumping have a substantial effect on the liquid flow, but that the liquid distribution at a given flow rate is fixed following this initial settling of the ore.

Table 2. Agreement between the images of the agglomerated ore where A was the first irrigation of the ore and B and C were subsequent irrigation cycles.

	Sample 1 Agreement (%)			Sample 2 Agreement (%)		
Time (minutes)	A_1 vs B_1	A_1 vs C_1	B_1 vs C_1	A_2 vs B_2	A_2 vs C_2	B_2 vs C_2
4	8.8	19.4	44.0	20.3	22.2	76.9
15	36.1	45.6	57.1	45.9	48.9	88.9
30	33.3	39.9	63.9	58.5	64.3	88.4
60	50.3	62.0	73.4	76.3	80.9	92.3
120	75.5	81.7	88.6	85.7	87.4	96.2
180	87.3	89.3	89.9	89.3	86.9	93.3

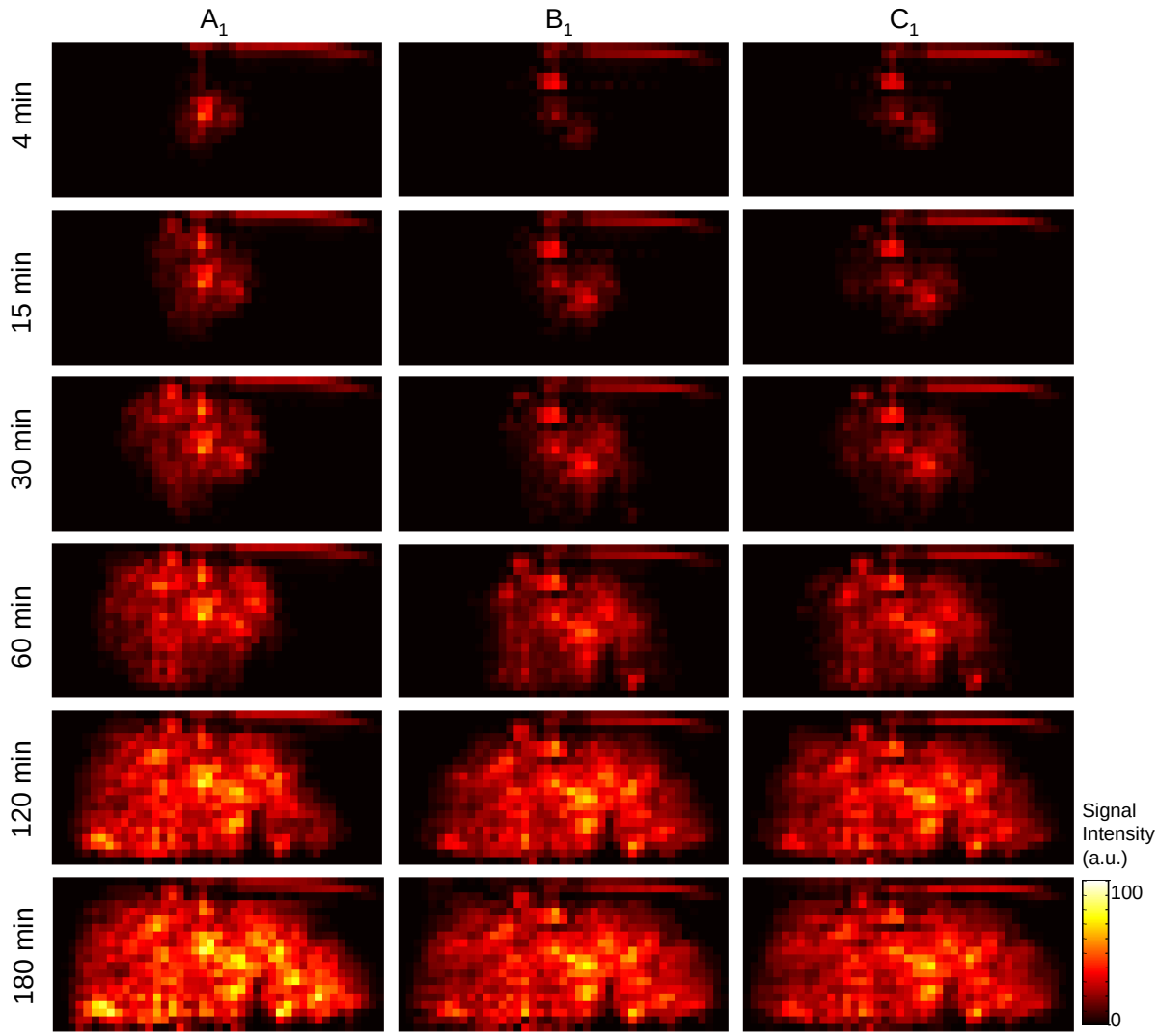

Figure 4. 2D y-z projections of the liquid infiltration from a single drip irrigation point into agglomerated ore sample 1. A_1 is the first irrigation of the ore and B_1 and C_1 are later runs that followed the initial irrigation and drying cycle.

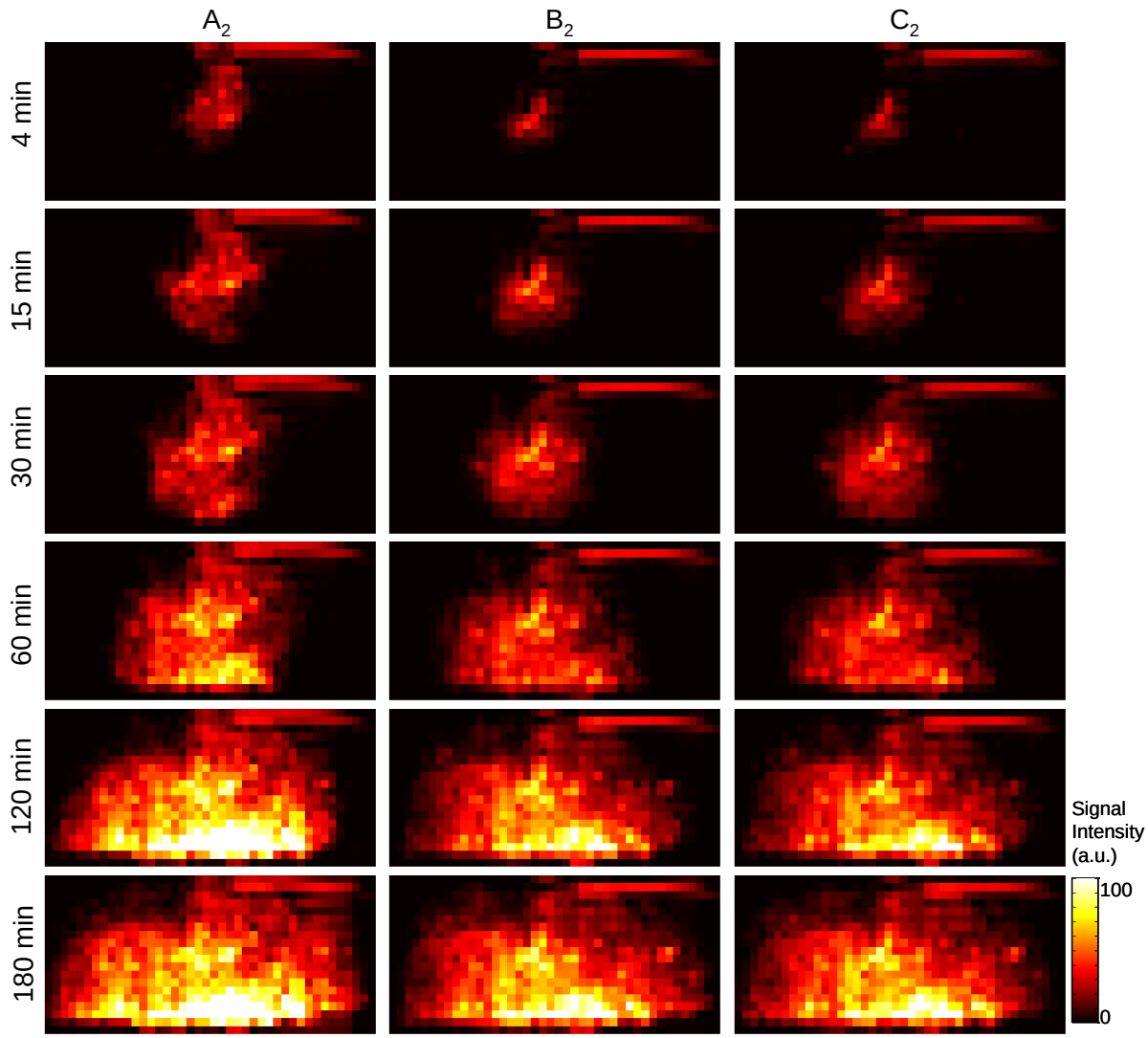

Figure 5. 2D y-z projections of the liquid infiltration from a single drip irrigation point into agglomerated ore sample 2. A_2 is the first irrigation of the ore and B_2 and C_2 are later runs that followed the initial irrigation and drying cycle.

2.1.2 D_2O tracer studies

In Figures 6 and 7, the 2D y-z projections of the series of three drip irrigation experiments performed on a further two agglomerated ore samples (I and II) are shown, comparing irrigation from the dry and wetted state. The projections presented for run C show the flow of the D_2O tracer into the already wetted bed. The percentages of the imaging region that had been infiltrated with the $GdCl_3$ doped water (runs A and B) or with D_2O (run C) as time progressed are presented in Table 3.

The wetting behaviour in the three runs of sample II had greater similarity than was the case for sample I because the liquid distribution in II was dominated by a channel of flow. Such

channels can be problematic in heap operation as they cause short circuiting of the liquid (O'Kane Consultants Inc., 2000). However, many similar trends in the liquid distribution exist between the two samples.

In both cases there was more rapid lateral spreading of the liquid in run A, the first irrigation of the ore, which resulted in run A having the largest distribution of signal for the first hour of irrigation. This is postulated to be because initially the fines in the ore bed were more evenly distributed as also observed in the repeat irrigation experiments. Hence shifting of the fines caused the lateral distribution of the irrigant liquid to be reduced in both dry and moist agglomerate beds, owing to reduced capillary action.

The slowest vertical infiltration rates occurred in run B when the pre-dried ore was irrigated for a second time. This contrasts with typical behaviour reported for soil drip irrigation (Brouwer et al., 1988), where the vertical infiltration rate is lower and the horizontal infiltration rate is higher in a wet system relative to a dry sample. When the ore bed is dry, the larger pores in the agglomerated ore are poor conductors of the liquid compared to the small pores in the fine ore packing. Therefore liquid flow in the dry ore (run B) is dominated by capillary suction as opposed to gravitational flow. The capillary suction decreases with increasing moisture content, so gravitational flow would be expected to become more dominant in the wet bed (runs A and C). The majority of the lateral dispersion of the liquid in run C would consequently be through diffusion into the stagnant liquid in the already wet ore instead. The results in Table 3 support this with run C having the least fluid exchange at all times due to reduced lateral infiltration of the liquid.

The amount of liquid that flows in channels versus the liquid that is present in thin rivulets or is held in the pores under capillary suction can be studied by considering the signal magnitude of the individual pixels in the 3D acquisition. The larger channels of liquid flow give off more signal as the volume of liquid per pixel is greater than in other areas. Therefore in order to ~~better~~ describe the type of liquid flow or retention in the ore bed, the pixels in the 3D acquisition of run B, performed after 4 hours of irrigation, were classified according to their signal magnitude. Thresholding was done at five signal magnitude levels: 0.5×10^5, 2×10^5, 4×10^5, 6×10^5 and 8×10^5. Pixels with signal greater than 8×10^5 were postulated to account for the centres of the main channels of liquid flow with the pixels of signal magnitude between 6×10^5 and 8×10^5 forming the rest of the large liquid channels. The lowest

value of 0.5×10^5 was the noise level. The liquid infiltration into the bed in the 3D acquisition of run C was then related to this original classification. Figure 8 and 9 are profiles which show the contribution of the signal classification ranges along the z axis. The overall liquid distributions are summarised in Table 4.

The majority of the liquid in run C, 54.8% and 57.8% respectively, flowed preferentially into pixels which had magnitude greater than 6×10^5, the larger liquid channel pixels. This is around 8% more than these pixels accounted for in the overall liquid distribution calculated from run B. These pixels were concentrated around the centre of the cell, in the region below the irrigation point. The larger liquid channel pixels accounted for less of the liquid as the lateral distance from the irrigation point increased. Consequently the liquid exchange at the end of run C is highest near to the irrigation point, shown in Figure 9. Similar concentration of the liquid flow in the region below the irrigation point was observed by van Hille et al. (2010) through effluent volume measurements. This result also agrees with the model predictions of Dixon (2003) who found that following the establishment of a wetted system, the majority of the liquid flows into channels, thereby limiting the lateral flow of solution.

The degree of exchange then decreased as the volumetric hold-up (signal magnitude) of the pixels decreased. The least amount of exchange was with the liquid in the pixels which have signal magnitude less than 2×10^5. Only 10.8% and 8.8% of the liquid in the D_2O tracer experiment flows into these pixels despite 15.4% and 14.4% of the liquid being held in these pixels in samples I and II respectively. The exchange that did occur was focussed in the central region of the bed, within the 30 mm either side of the irrigation point. These low signal magnitude pixels would most likely have contained stagnant liquid held in the intra- and fine inter-particle pores. Therefore any exchange with this liquid would have been determined by diffusion rather than flow. A longer observation time may have been required to see significant exchange with the freshly irrigated liquid in these pixels.

The proportion of the liquid held in the lower intensity pixels increased as the horizontal distance from the irrigation point increased, as can be seen in part (a) of Figures 8 and 9. For example, the pixels of signal magnitude less than 2×10^5 accounted for less than 12% of the liquid in the centre of the cell, but more than 50% (maximum of 76%) of the liquid at the edges. Therefore the percentage of the liquid that had been replaced by the end of run C,

shown in Figure 9, is as low as 2% at the edges of the ore region, much lower than the circa 90% maximum exchange that occurred closer to the irrigation point.

The region of lowest signal intensity was in the top corners of the imaging region in all of the experiments. This is most obvious in runs A and C where there was almost no signal present in these regions. The particle size of the agglomerated ore did not allow for sufficient capillary suction to enable pure horizontal or upward wicking of the liquid when the system is not dry. Such limited liquid exchange could cause poor local recovery of the mineral in a heap leach because of transport issues, poor microbial colonisation, and other problems such as jarosite precipitation caused by high local acid consumption (van Hille et al., 2010). This issue is expected to be more pronounced in full scale operation than is observed in the 100 mm imaging region of the MRI and is thus a major disadvantage of drip irrigation.

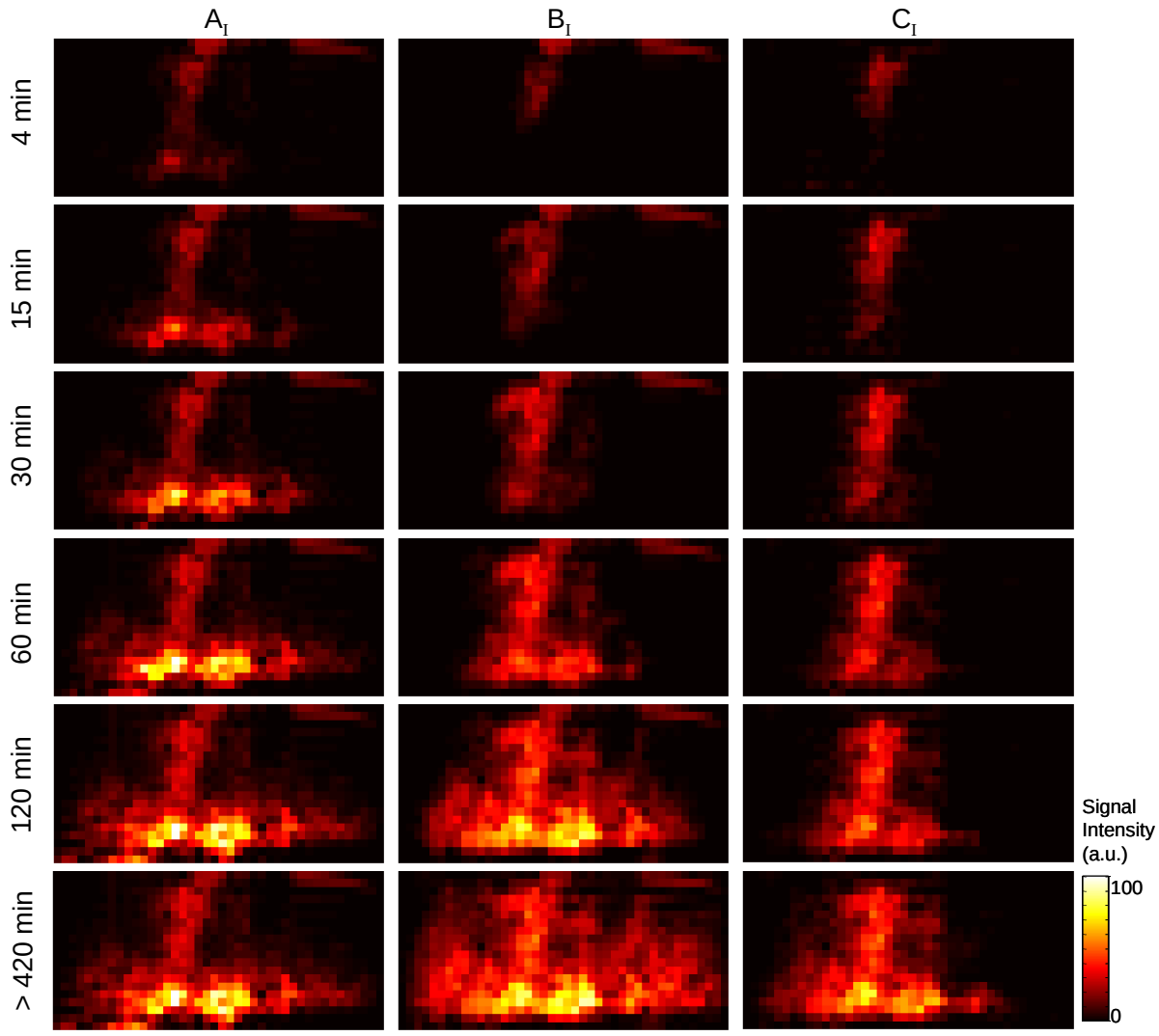

Figure 6. 2D y-z projections of the liquid infiltration from a single drip irrigation point into sample I. Run A_I is when the moist D_2O agglomerated ore was irrigated with doped water. For run B_I the ore had been dried overnight and was irrigated with doped water. Run C_I shows the D_2O path following a swap in the liquid feed from the doped water solution in run B_I once steady state had been reached.

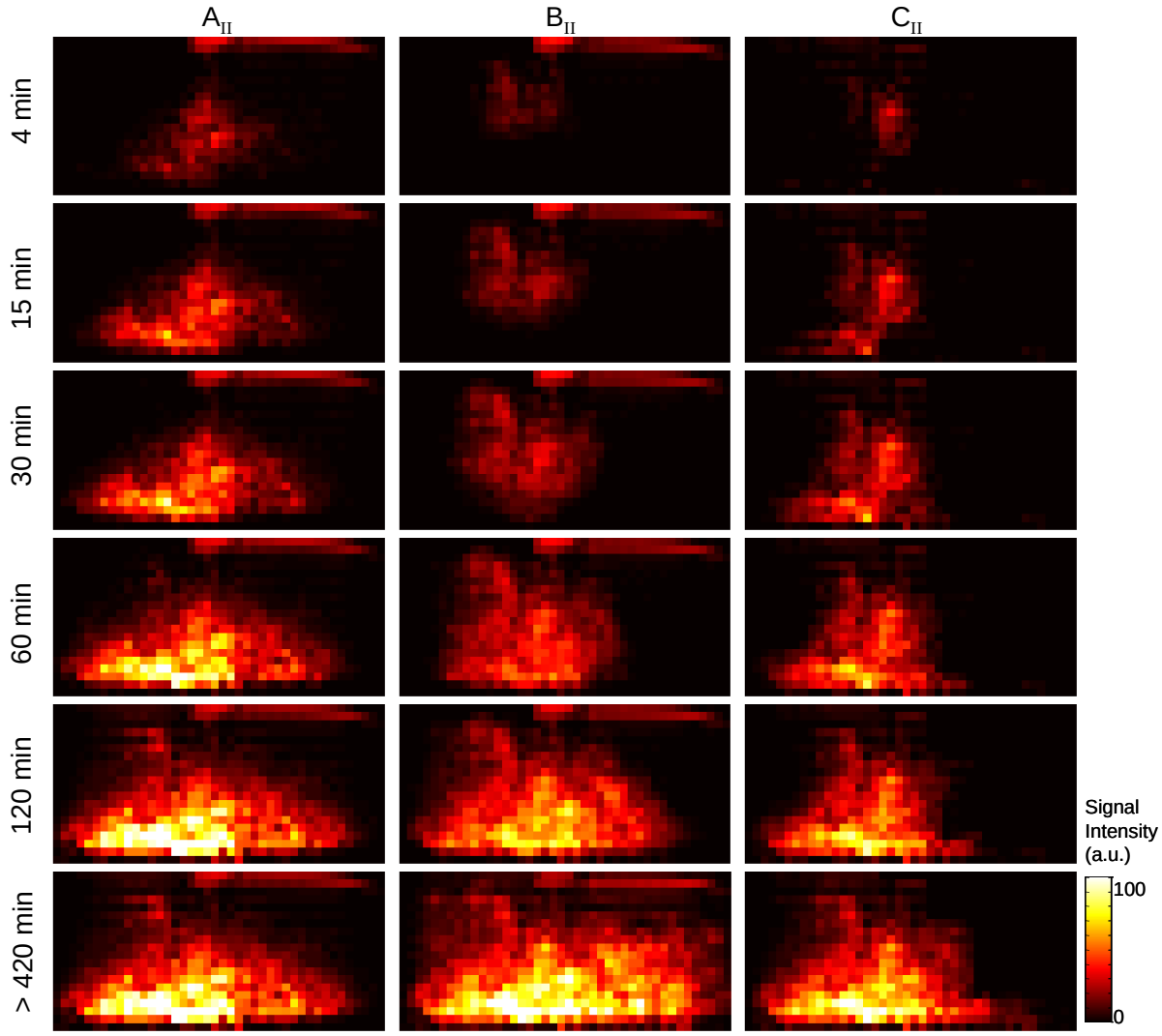

Figure 7. 2D y-z projections of the liquid infiltration from a single drip irrigation point into sample II. Run A_{II} is when the moist D_2O agglomerated ore was irrigated with doped water. For run B_{II} the ore had been dried overnight and was irrigated with doped water. Run C_{II} shows the D_2O path following a swap in the liquid feed from the doped water solution in run B_{II} once steady state had been reached.

Table 3. Percentage of the imaging region in 2D y-z projections of the D_2O agglomerated ore that contained the $GdCl_3$ doped water (runs A and B) or the D_2O (run C).

	Sample I liquid filled area (%)			Sample II liquid filled area (%)		
Time (minutes)	A_I	B_I	C_I	A_{II}	B_{II}	C_{II}
4	10.4	3.7	4.6	15.9	6.0	5.3
15	20.7	10.2	10.1	31.4	15.3	16.7
30	30.0	18.7	16.7	37.8	27.7	26.6
60	43.8	35.8	26.8	50.0	44.9	33.1
120	52.8	63.5	33.4	59.6	61.9	40.2
> 420	53.2	84.2	50.5	62.0	83.7	52.3

Table 4. Location of the liquid in run C (exchanged liquid) relative to the signal magnitude of the pixels in the 3D acquisition of run B at steady state (overall liquid distribution).

Pixel signal magnitude in run B	Sample I		Sample II	
	Overall liquid distribution (%)	Exchanged liquid (%)	Overall liquid distribution (%)	Exchanged liquid (%)
$0 - 2\times10^5$	15.4	10.8	14.4	8.8
$2\times10^5 - 4\times10^5$	19.1	16.7	9.7	16.3
$4\times10^5 - 6\times10^5$	18.2	17.7	26.2	17.1
$6\times10^5 - 8\times10^5$	15.5	16.8	15.0	16.2
$> 8\times10^5$	31.9	38.0	34.7	41.6

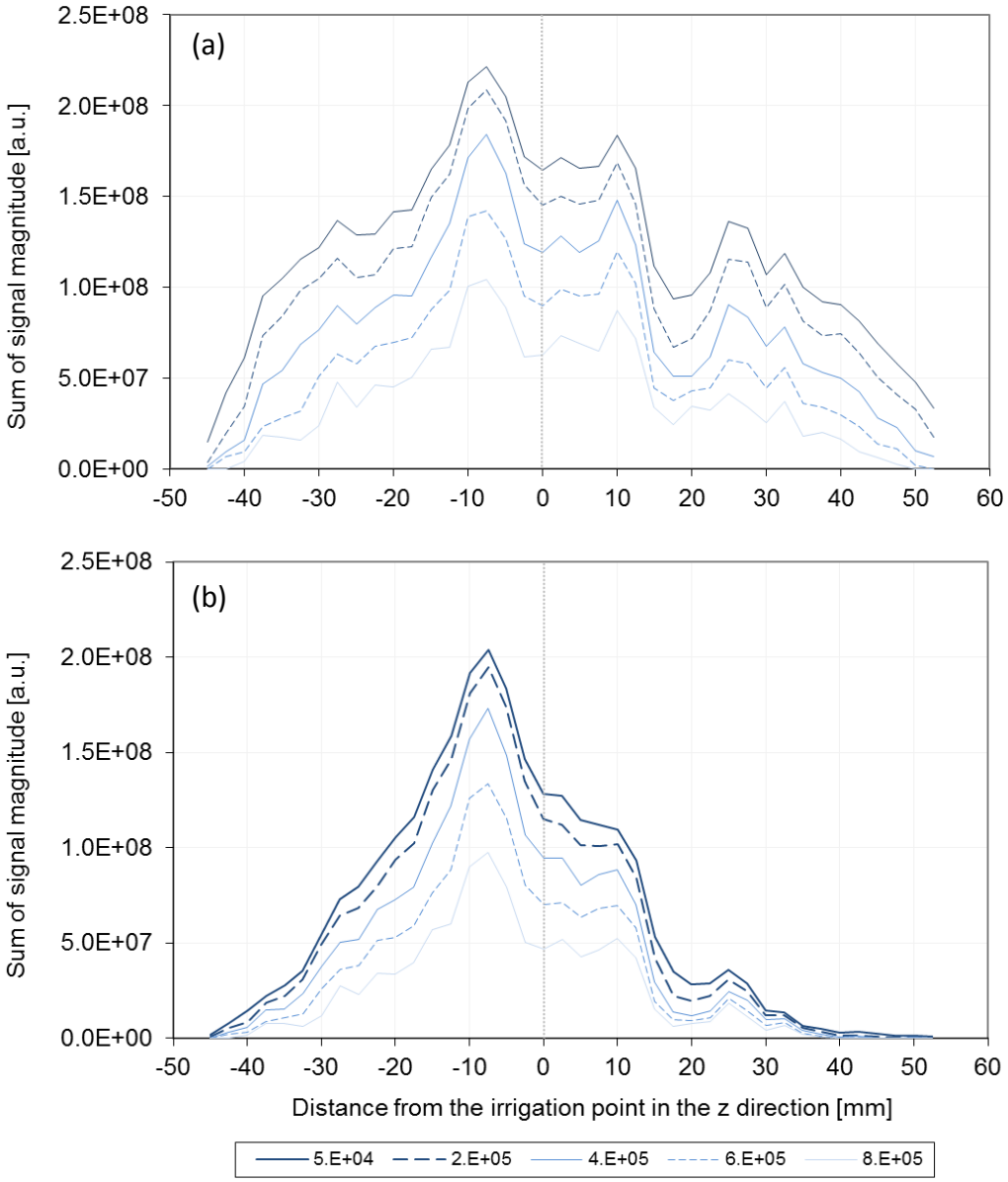

Figure 8. The pixels from the 3D acquisition (after four hours) of run B_I on the first D_2O agglomerated ore sample are classified according to their signal magnitude, where (a) shows the profiles of the sum of the signal above given values. The signal from the liquid in run C_I that flows into these pre-classified pixels is presented as profiles in (b).

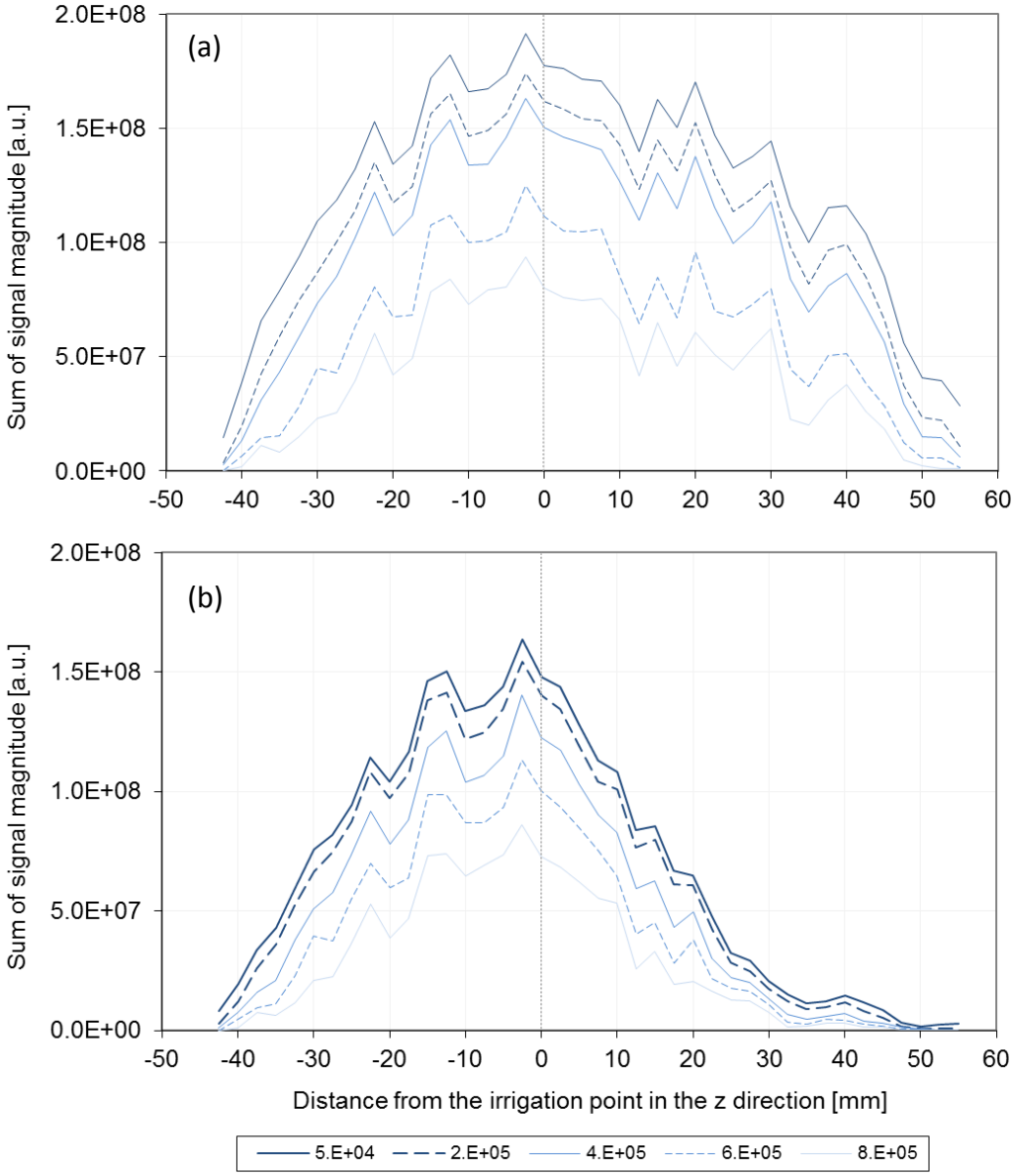

Figure 9. The pixels from the 3D acquisition (after four hours) of run B_{II} on the second D_2O agglomerated ore sample are classified according to their signal magnitude, where (a) shows the profiles of the sum of the signal above given values. The signal from the liquid in run C_{II} that flowed into these pre-classified pixels is presented as profiles in (b).

3.2 Bioleach "ore-slice" box reactor

3.2.1 Solution flow and moisture content

The results of the two methods by which the liquid distribution was assessed in the box, namely effluent volume measurements and in-bed sampling, are presented in Figures 10 and 11. The majority of the solution flowing out of the bed (average of 97.7%) was collected from the first six ports, representing a horizontal dimension of 280 mm over a vertical

distance of 1200 mm. This provided evidence of some lateral distribution from the point source. Port 5 in particular accounted for 62% of the total flow. This indicated the existence of a preferential flow path(s) in the bed as described by Rossi (1990), Decker and Tyler (1999) and O'Kane et al. (2000). It also supported the assumption that wall effects did not have any significant effect on the liquid distribution.

The in-bed sampling showed that there was an increase in the average moisture content of the bed over time, from 8.6% (day 24) to 10.1% (day 49) to 10.7% (day 63) up to 12.2% (day 83). The ore was initially (day 24) wet evenly with little variation between the zones. This can be attributed to the initial irrigation procedure from multiple ports as well as the fact that capillary suction is stronger at lower moisture content. Zone G had the highest moisture content on day 49, a result of the downwards movement of fluid under gravity, whilst zone C was the driest. Thus a gradient in the degree of wetness developed from the bottom left corner (high) to the top right (low). The moisture distribution was less uniform on the last two sample days. On day 63, the biggest increases in moisture content were for zones A, E and H to 16.1, 17.1 and 12.5% respectively, indicating that there was more lateral distribution of liquid within the first two thirds of the bed. The high moisture content in E and H corresponds to the position of port 5 and hence the preferential flow path. One anomaly was the low moisture content value for zone D on day 63, given as 5.1%. This value was expected to be higher as solution flow through the outlet ports below this zone was also high. However, the low value may have been due to the changing solution flow paths along the pore network within the box heap. The moisture content of the bed on day 83 had increased further with depth and laterally, corresponding to the lateral and downward expansion of the water saturation observed by Yarwood et al. (2006). The highest moisture content attained was 19.2% in zone E and the average moisture content increased to 12.2%.

Therefore throughout the experiment, the wettest zones in the ore bed were those located in the vertical regions closest to the irrigant source that was fed with liquid that flows under gravity from the irrigation point, whereas the driest zones of the bed were in the top right corner (zones B, C and F), regions that would only have been wetted by the lateral movement of the liquid under capillary suction. The same trend was observed for the smaller scale MRI experiments. Drip emitters are typically placed at intervals of 0.5 to 1.5 meters (Kappes, 2002), designed to each cover an area of approximately one square metre (Bartlett, 1998). The poor wetting observed in zones B, C and F thus might not occur at the closer emitter

spacing, but results similar to those observed in this study would be expected if the emitters were spaced at the larger distances.

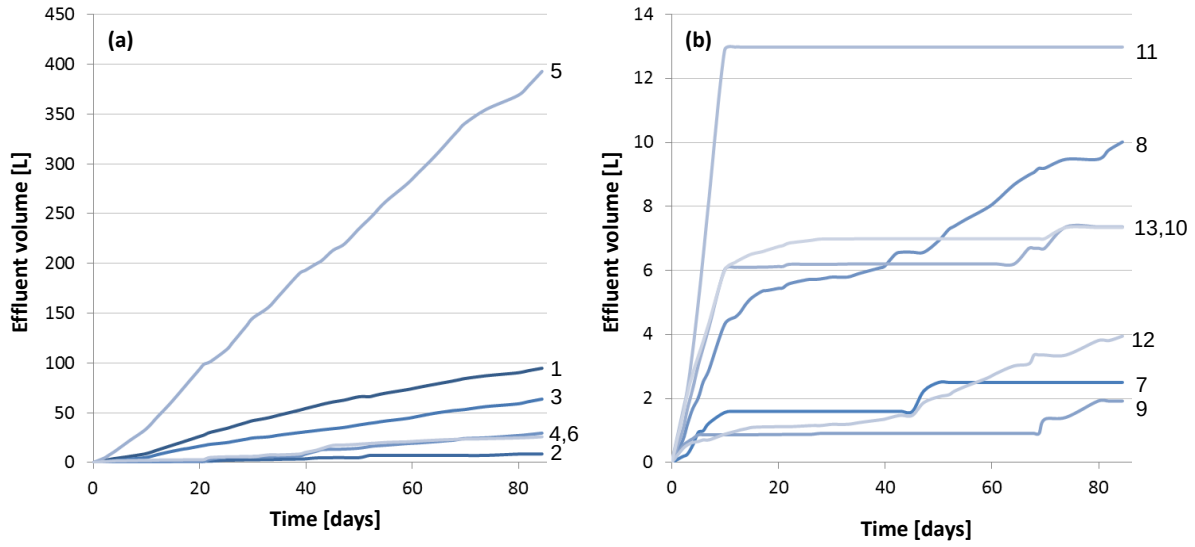

Figure 10. Cumulative effluent liquid volumes collected from ports 1 to 13 during the bioleaching of the low grade copper bearing ore in the box reactor, displayed against either a (a) large or (b) small effluent volume range.

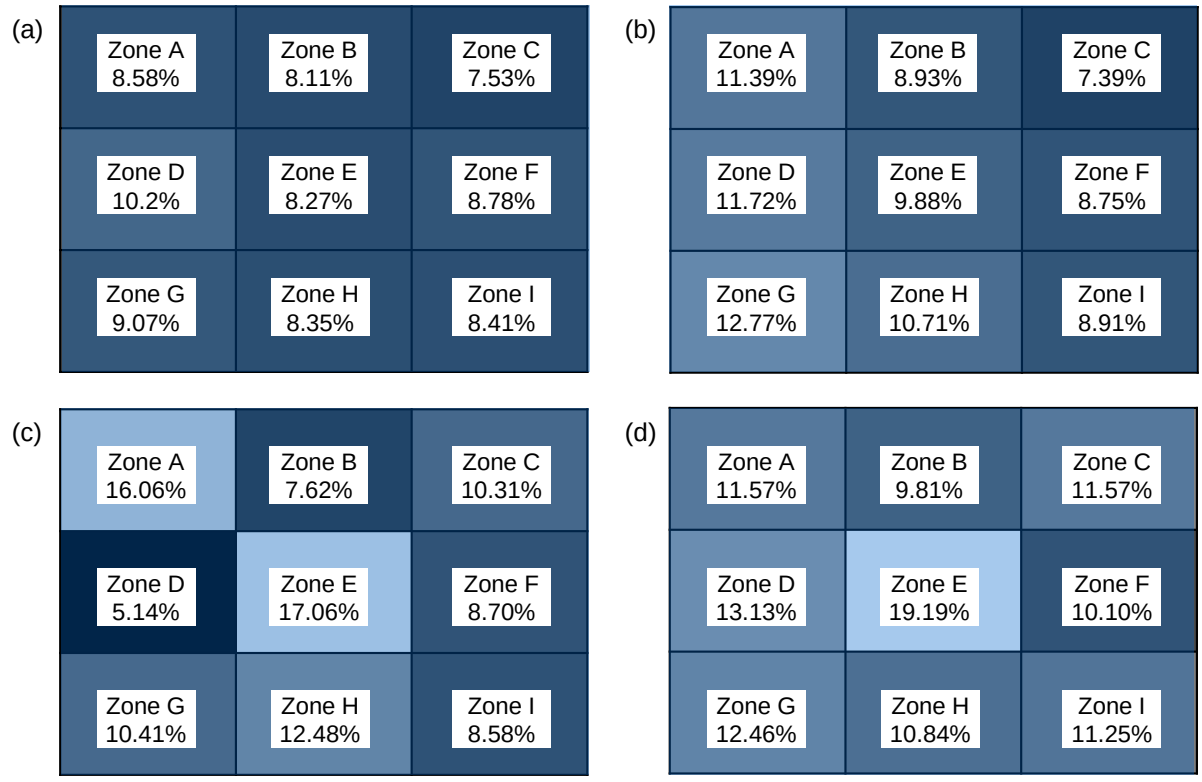

Figure 11. Moisture content in the different zones of the box reactor expressed as a weight percentage on days (a) 24, (b) 49, (c) 63 and (d) 83.

3.2.2 Bioleaching performance

Figure 12 presents the copper recovery data from the individual effluent ports as well as the total copper extraction attained which gives a measure of the leach and Figure 13 gives the effluent pH and redox potential measurements. The majority of the copper liberation was during the acid-wash stage at a rapid rate of 1.30 g/day over the first 10 days. This was due to the dissolution of the available acid-soluble copper from oxides and secondary sulphides, a conclusion that is supported by the higher effluent pH and relatively low redox potential during this period compared to the feed (pH 1.15, redox potential ~380 mV) and post-inoculation measurements. Thereafter, the copper extraction rate decreased, continuing at a constant rate of 0.14 g/day for the duration of the leaching process to yield 18% copper extraction after 90 days. During this period the effluent pH remained marginally above the feed value of 1.15. Towards the end of the acid wash the redox potential had stabilised at close to 400, but following the bed inoculation it increased to circa 700 as a result of microbial oxidation of the ferrous iron.

The rate and extent of copper extraction is dependent on factors such as the operation temperature regime, solution chemistry, microbial species present, ore mineralogy and the accessibility of leach solution to the exposed mineral surface (Watling, 2006). According to Watling (2006), 40% of available chalcocite and bornite is typically recovered during the first 10 days of leaching, along with 80% of the available copper oxides. This coincides with the rapid copper extraction during the first 10 days from the ore-slice contained in the box reactor. The low final copper extraction value can be attributed to the short leach duration (83 days) for a chalcopyrite containing ore and the large proportion of gangue material with which the leach solution was contacted. Furthermore, the ambient operation was not ideal for the leaching of the chalcopyrite (28.4% of the copper mineral) which is better leached at thermophilic bioleaching temperatures (Watling, 2006).

The largest quantities of copper were extracted via ports 1, 3, 5, 8 and 11, contributing 12.0, 6.5, 48.7, 5.9 and 7.5% of the extracted copper. Thus the port which expelled the largest volume of leach solution was responsible for the recovery of the majority of the copper. Since the copper extraction rate is a function of the available exposed mineral surface contacted by the leach solution (Rossi, 1990), the observed copper removal confirms that most of the liquid-ore contacting took place within the first two thirds of the ore bed, i.e. zones A, D, E, G and H.

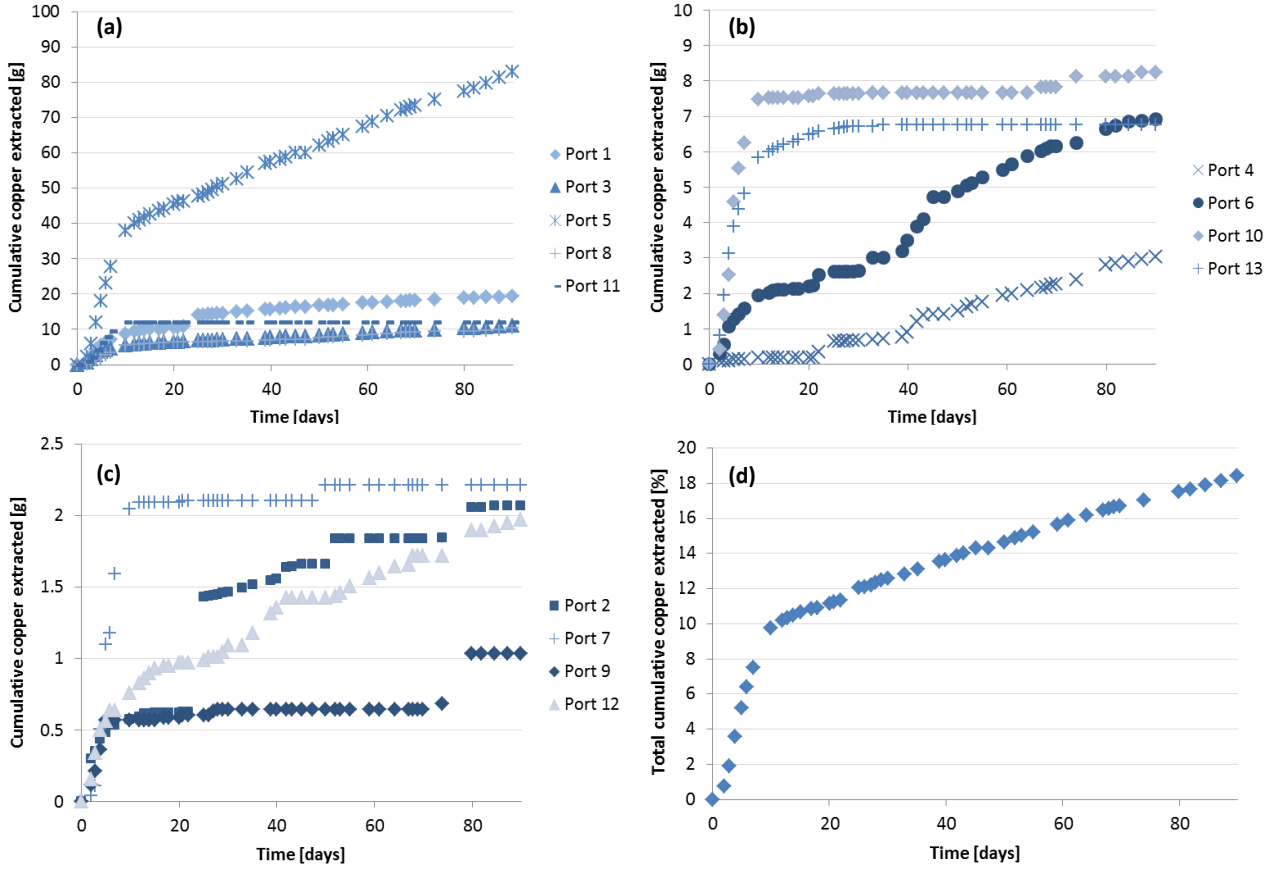

Figure 12. Cumulative copper removal in the box reactor as a function of time, given (a) - (c) for each of the 13 effluent collection ports and as (d) an overall total percentage extraction based on the head grade ore assay.

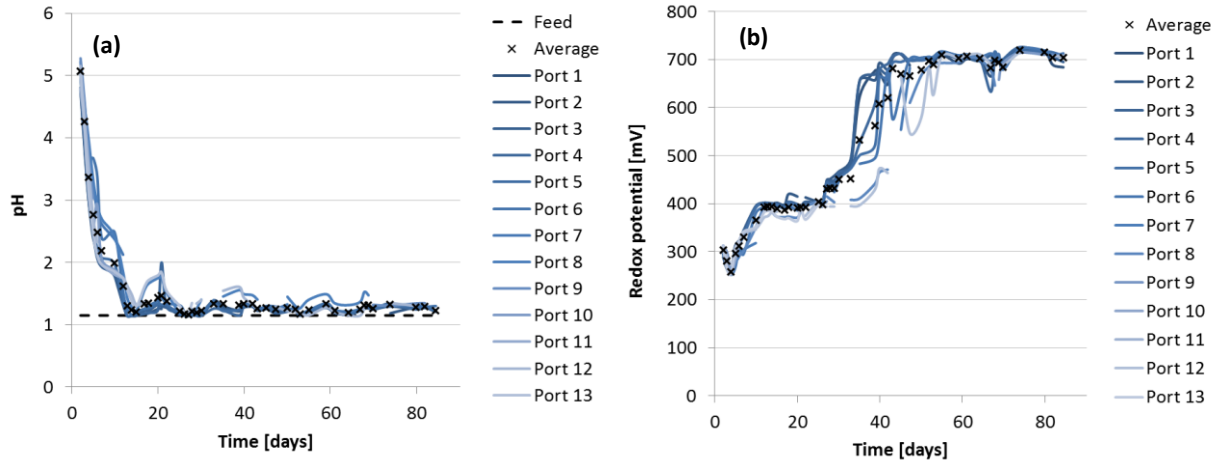

Figure 13. Effluent (a) pH and (b) redox potential as a function of time. Gaps in the data occur when the port effluent volumes were too small to allow for pH and redox readings.

3.2.3 Microbial propagation and colonisation

Microbial cells eluted in the PLS and the cell concentrations within different locations of the ore bed were monitored to assess the relationship between fluid flow channels and the transportation of micro-organisms within heap environments.

Figure 14 shows the cumulative planktonic cells eluted from the ore bed as a function of time for outlet ports 1, 2, 3, 4, 5, 6 and 8. The cells present within the other ports were either very low in number or not detectable under the microscope. Combined with the low effluent volumes collected from these ports, their contribution to the total was negligible. Microbial cells were detected in the eluted solution on the day 28, one day after inoculation. Therefore some cells were washed out of the bed without attachment and growth within the heap. The initial cell concentrations in the PLS ranged from below the detection limit to 9.4×10^5 cells/ml. Between day 28 and 38, the cumulative number of cells exported from the heap was very low. From day 39 onwards, the cell exportation rate increased gradually. This is postulated to be due to an increase in cell numbers within the ore bed as a result of microbial growth. The majority, approximately 68%, of the total cells eluted were removed from the system via port 5. This, like the copper recovery, corresponds to the highest outlet flow being through port 5. This may result from the cell numbers being densest within the wettest region, or cell detachment being greatest in high flow rate regions as was found by Chiume et al. (2012), or both.

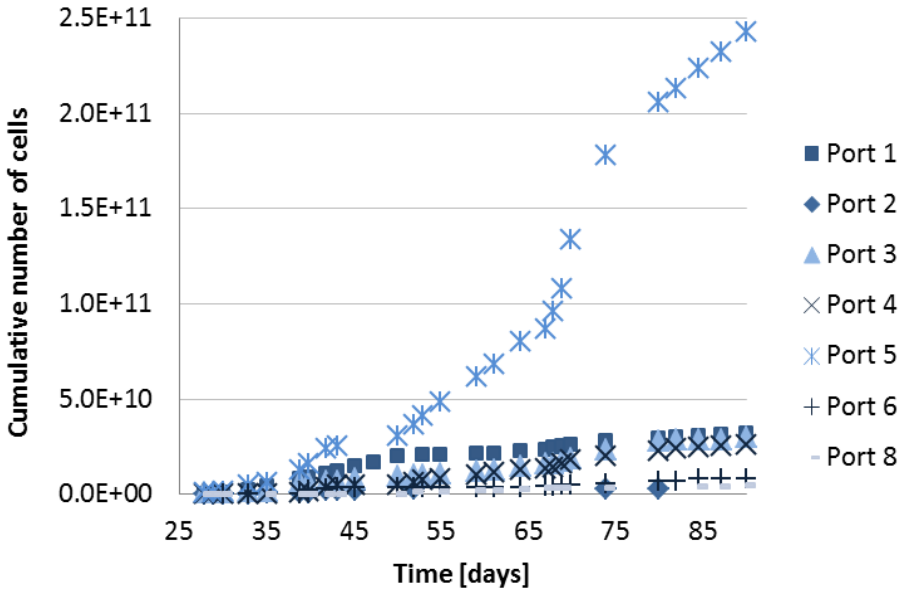

Figure 14. Trend in the cumulative number of cells exported in the leachate passing through the box reactor heap given for outlet ports 1, 2, 3, 4, 5, 6 and 8.

The cell density plots in Figure 15 are indicative of the spatial distribution of the micro-organisms within the system on the measurement days. A clear increase in cell density, and hence microbial growth and retention, was observed across the whole ore bed over time. The average cell density rose from 1.4×10^{10} cells/kg ore at 22 days post inoculation to 4.5×10^{10} cells/kg ore (36 days after inoculation) to 6.7×10^{10} cells/kg ore (56 days after inoculation). On all three measurement days the highest cell densities were found below the irrigation point on the left vertical region of the bed (zones A, D and G) which is similar to the movement of cells reported by Yarwood et al. (2006) in their studies of microbial growth in unsaturated sand beds. This can be attributed to a higher degree of liquid-mineral contacting in these regions as result of the preferential distribution of micro-organisms near the point source of irrigation, as found by Seifert and Engesgaard (2007) in their studies of bioclogging, and along the preferential flow paths evidenced by the moisture content data (Decker and Tyler, 1999; O'Kane Consultants Inc., 2000; Rossi, 1990). The cell densities also increased with depth. This can be attributed to the downward migration of micro-organisms as a result of cell detachment and fluid flow (Chiume et al., 2012; Seifert and Engesgaard, 2007). As was identified with respect to the PLS cell counts, this parallels the increased wetness of the ore bed in the lateral and downward direction as a function of time. The downward movement of the cells could also be due to micro-organisms' search for favourable leaching conditions (Rossi, 1990; van Loosdrecht et al., 1990). Petersen and Dixon (2007) also reported increasing cell numbers with time and decreasing depth within their column studies. The lowest cell densities were located on the right side of the bed with zones C and F remaining at levels below the lower detection limit of the microscopic cell counting method (10^5 cells/ml $\approx 5\times10^7$cells/kg ore) for the duration of the run. This implies that lack of liquid exchange in regions wetted through capillary action, as evidenced by the MRI experiments, may result in portions of a heap remaining un-colonised which could lead to inefficient leaching of these regions of an ore bed. The unsaturated condition is a requirement for leaching because oxygen is required by the iron- and/or sulfur oxidising microorganisms. Thus there is expected to be a moisture content threshold beyond which oxygen limitation detrimentally affects the microbial population. The observed correlation between high moisture content and cell densities in the bed however indicate that oxygen limitation was not a concern at the moisture levels that existed within the ore bed.

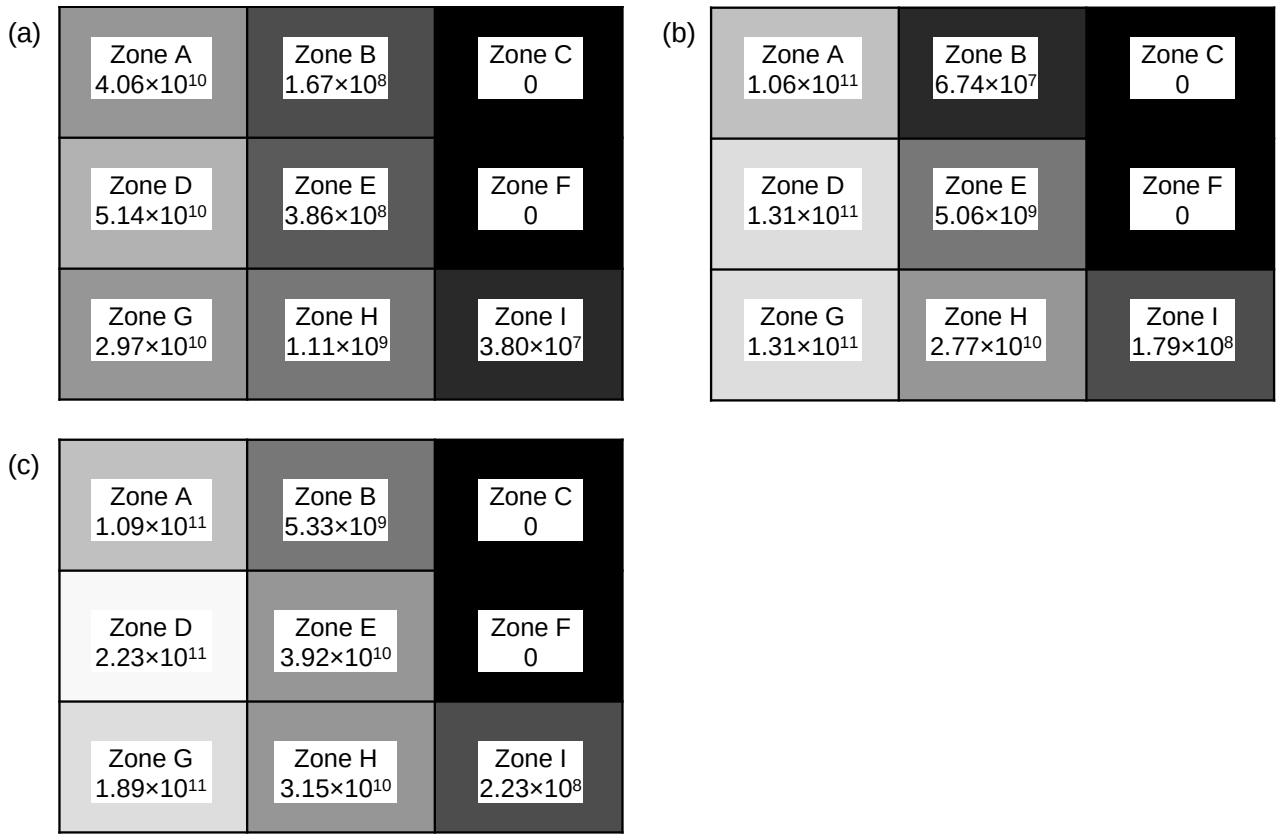

Figure 15. Cell densities in each of the nine zones determined by mechanical detachment and microscopic analysis of the ore samples removed from the ore bed on day (a) 49, (b) 63 and (c) 83.

CONCLUSIONS

In both the MRI experiments and in the larger "ore-slice" box reactor system, the liquid distribution was observed to increase laterally with depth. This is because the high moisture regions were wetted by liquid channels that flowed under gravity, whereas the upper regions of the ore bed were wetted through capillary movement of liquid. The MRI data showed that slumping of the ore during an initial irrigation cycle permanently altered the liquid flow path which subsequently remained stable. Specifically, washing of the fines towards the base or out of the bed resulted in limitation of the lateral distribution of the leach solution which suggests the need for binding agents during the agglomeration process. Following the establishment of a wetted bed, the majority (just less than 60%) of the freshly irrigated solution entered directly into the larger established channels of flow. This meant that liquid exchange was maximum in the region below the irrigation point. The degree of liquid exchange decreased as the volumetric hold-up of a region decreased, with the least exchange occurring with regions (pixels) which were presumed to contain stagnant liquid held in pores.

Almost no exchange occurred in the areas of lowest liquid content at the upper corners of the cell. Hence poor to no liquid exchange occurred in regions of the ore bed that had been wetted through capillary forces.

The wettest zones in the box reactor were those located in the vertical regions closest to the irrigant source while the driest zone of the bed at the end of the experiment was in the top right corner, the furthest lateral position from the irrigation point where wetting must be by capillary action. The liquid flow under gravity was focussed in the half of the bed closest to the irrigation point with 97% of the effluent liquid collected through the first six of 13 ports, more than half of which was expelled via a preferential flow channel at port 5. The cell densities in the different regions paralleled the moisture content, with the highest densities found below the irrigation point and towards the base of the reactor whereas the top right zones remained at undetectable cell counts. Thus poor liquid exchange occurred in regions between irrigation points which were wetted through capillary suction and not gravitational flow following the establishment of a steady state liquid distribution. It is apparent that this limited liquid exchange was severely limiting to microbial transport and hence the colonisation of these areas. The majority of the copper extracted from the ore bed was also removed from the areas with the higher fluid throughput. This can be attributed to both good mineral-liquid contacting in these regions as well as the higher bioleaching cell densities. In summary, a clear correlation was found between the wettest regions of the ore bed and the highest cell density and copper recoveries. Further these wettest regions result from a combination of preferential flow channels and gravity flow. Lateral fluid exchange is governed by capillary action which is influenced by the distribution of fines in the ore bed. Optimal leaching of the ore bed will require excellent distribution of the liquid phase and appropriate liquid exchange.

ACKNOWLEDGEMENTS

The authors would like to acknowledge and thank BHP Billiton, the Cambridge Commonwealth Trust, Trinity College Cambridge, the South African Research Chairs Initiative of the Department of Science and Technology, the National Research Foundation and Cape Biotech Trust/Technology Innovation Agency of South Africa (TIA) for their sponsorship and support of components of this project.

REFERENCES

Africa, C., Harrison, S.T.L., Becker, M., van Hille, R.P., 2010. In-situ investigation and visualisation of microbial attachment and colonisation in a heap bioleach environment: The novel biofilm reactor. Miner. Eng., 23: 486-491.

Bartlett, R.W., 1998. Solution Mining: Leaching and Fluid Recovery of Materials. Routledge, 443 pp.

Bouffard, S.C. and Dixon, D.G., 2001. Investigative study into the hydrodynamics of heap leaching processes. Metall. Mater. Trans. B, 32(5): 763-776.

Brouwer, C., Prins, K., Kay, M. and Heibloem, M., 1988. Irrigation Water Management: Irrigation Methods. Training Manual Number 5. Food and Agriculture Organization of the United Nations, Rome, Italy.

Chiume, R., Minnaar, S.H., Ngoma, I.E., Bryan, C.G. and Harrison, S.T.L., 2012. Microbial colonisation in heaps for mineral bioleaching and the influence of irrigation rate. Miner. Eng., 39: 156-164.

De Andrade Lima, L.R.P., 2006. Liquid axial dispersion and holdup in column leaching. Miner. Eng., 19: 37-47.

Decker, D.L. and Tyler, S.W., 1999. Hydrodynamics and solute transport in heap leach mining. In: D. Kosich and G. Miller (Eds.), Closure, Remediation & Management of Precious Metals Heap Leach Facilities.

Dixon, D.G., 2003. Heap leach modeling – the current state of the art. In: C.A. Young et al. (Eds.), H*ydrometallurgy 2003, Volume 1: Leaching and Solution Percolation*. The Minerals, Metals and Materials Society, Warrendale, Pennsylvania, pp. 289-314.

Fagan, M.A., Sederman, A.J., Harrison, S.T.L. and Johns, M.L., 2013. Phase distribution identification in the column leaching of low grade ores using MRI. Miner. Eng., 48: 94-99.

Fagan, M.A., Sederman, A.J. and Johns, M.L., 2012. MR imaging of ore for heap bioleaching studies using pure phase encode acquisition methods. J. Magn. Reson, 216: 121-127.

Ghauri, M.A., Okibe, N. and Johnson, D.B., 2007. Attachment of acidophilic bacteria to solid surfaces: The significance of species and strain variations. Hydrometallurgy, 85(2–4): 72-80.

Ilankoon, I.M.S.K. and Neethling, S.J., 2012. Hysteresis in unsaturated flow in packed beds and heaps. Miner. Eng., 35: 1-8.

Kappes, D.W., 2002. Precious Metal Heap Leach Design and Practice. Kappes, Cassiday & Associates, Reno, Nevada, 25 pp.

Komadel, P. and Stucki, J.W., 1988. Quantitative assay of minerals for Fe2+ and Fe3+ using 1,10-Phenanthroline: III. A rapid photochemical method. Clays Clay Miner., 36(4): 379-381.

Lin, C.L., Miller, J.D. and Garcia, C., 2005. Saturated flow characteristics in column leaching as described by LB simulation. Miner. Eng., 18(10): 1045-1051.

O'Kane Consultants Inc., 2000. Demonstration of the application of unsaturated zone hydrology for heap leaching optimization. Industrial Research Assistance Program Contract # 332407(628-1).

Petersen, J. and Dixon, D.G., 2007. Principles, mechanisms and dynamics of chalcocite heap bioleaching. In: D.E. Donati and W. Sand (Eds.), Microbial Processing of Metal Sulphides. Springer, pp. 193-218.

Rodriguez, Y., Ballester, A., Blazquez, M.L., Gonzalez, F. and Munoz, J.A., 2003. Study of bacterial attachment during the bioleaching of pyrite, chalcopyrite, and sphalerite. Geomicrobiol. J., 20(2): 131-141.

Rossi, G., 1990. Biohydrometallurgy. McGraw-Hill, Hamburg, 609 pp.

Seifert, D. and Engesgaard, P., 2007. Use of tracer tests to investigate changes in flow and transport properties due to bioclogging of porous media. J. Contam. Hydrol., 93(1–4): 58-71.

van Hille, R.P., van Zyl, A.W., Spurr, N.R.L. and Harrison, S.T.L., 2010. Investigating heap bioleaching: Effect of feed iron concentration on bioleaching performance. Miner. Eng., 23(6): 518-525.

van Loosdrecht, M.C.M., Lyklema, J., Norde, W. and Zehnder, A.J.B., 1990. Influence of interfaces on microbial activity. Microbiol. Rev., 54(1): 75-87.

Watling, H.R., 2006. The bioleaching of sulphide minerals with emphasis on copper sulphides - A review. Hydrometallurgy, 84(1-2): 81-108.

Wu, A.X., Yin, S.H., Yang, B.H., Wang, J. and Qiu, G.Z., 2007. Study on preferential flow in dump leaching of low-grade ores. Hydrometallurgy, 87(3-4): 124-132.

Yarwood, R.R., Rockhold, M.L., Niemet, M.R., Selker, J.S. and Bottomley, P.J., 2006. Impact of microbial growth on water flow and solute transport in unsaturated porous media. Water Resour. Res., 42(10): W10405.